

Evolution of supernova remnants in the interstellar medium with a large-scale density gradient

II. The 2-D modelling of the evolution and X-ray emission of supernova remnant RCW86

O. Petruk

Institute for Applied Problems in Mechanics and Mathematics, NAS of Ukraine, 3-b Naukova St., Lviv, 290601, Ukraine
Petruk@lms.lviv.ua

Received ...; accepted ...

Abstract. The results of the 2D modelling of Supernova remnant (SNR) RCW86 are given. Models of this remnant, which for the first time interpret the anisotropy of surface brightness as a result of the evolution of adiabatic SNR in the interstellar medium with a large-scale gradient of density, are considered. Estimations on the basic characteristics of RCW86 and the surrounding medium which follow from these models are found. It is shown that the observed surface brightness distribution of RCW86 may be obtained in the both proposed up till now models with different initial assumptions: one about a Supernova explosion in 185 A.D. and another about an explosion in the OB-association. In order to obtain the observational contrast of surface brightness it is necessary to have a medium with the characteristic scale of nonuniformity 11 pc if the age of RCW86 is 1800 years or 20 – 25 pc when the SNR is distant from us on 2.8 kpc. The preshock density contrast between the southwestern and northeastern parts of RCW86 is in range 3.5 – 4.5.

Key words: ISM: supernova remnants – ISM: individual objects: RCW86 – hydrodynamics – X-rays: interstellar

1. Introduction

Supernova remnant (SNR) G315.4-2.3 (RCW86, MSH14-63) is the result of a supernova explosion which is regarded as one of the most possible candidates for the "guest star" of 185 A.D. according to Chinese manuscripts (Clark & Stephenson 1977).

Chin & Huang (1994), Schaefer (1995) argue that the "guest star" in 185 A.D. was not a Supernova (SN). Then it is not right to assume that the age of RCW86 is $t =$

1800 years although the SNR might be a relatively young remnant because it has a radial oriented magnetic field (Milne 1987) like Tycho, Cas A and Kepler SNRs (Strom 1994).

The SN progenitor might be a member of OB-association. In this case we may expect the SN to have been of type II, but it could not be born in 185 A.D. since the SNR has much bigger size than the expected one if it is situated at the distance $d \approx 2.8$ kpc obtained from the kinematic survey of ionized H (Rosado et al. 1996).

From the ratio H_α/H_β for optical filaments Ruiz (1981) estimates the distance to the SNR as $d \approx 1$ kpc.

RCW86, as radio source MSH14-63, was identified by Hill (1967). $\Sigma - D$ relation yields an estimation on the distance to the SNR $d = 2 \div 3.2$ kpc (Milne 1970), but the possible range is, nevertheless, $d = 1 \div 10$ kpc (Strom 1994).

Both the radio and the X-ray observations reveal that the shape of RCW86 is close to a spherical one with the size $43' \times 40'$ (at frequency 843 MHz) and is of a shell-like type with the approximately axis-symmetrical surface brightness distribution and higher emission in the southwest (SW) part of the SNR (Caswell et al. 1975, Pisarski et al. 1984, Claas et al. 1989, Whiteoak & Green 1996). The brightest optical filaments coincide with the maximums of emission in radio and X-ray bands (van den Bergh 1978, Pisarski et al. 1984).

The important results in investigation of RCW86 were caused by analyzing the spectral properties of X-ray emission from this SNR. The first soft X-ray observations were reported and interpreted by Naranan (1977). Winkler (1978), having used hard X-ray data, showed that the observed spectrum might be explained as thermal, with two bremsstrahlung components (from the forward and reverse

shock waves) with the temperatures $T_{\text{low}} \approx 0.22$ keV and $T_{\text{high}} \geq 5$ keV.

The first map of the X-ray surface brightness distribution of RCW86 was presented by Pisarski et al. (1984) (EINSTEIN observatory). The authors noted that higher emission from the SW part might be caused by the interaction of the shock wave with the interstellar medium (ISM) with a density 2-3 times higher than the average. The one temperature fitting of the spectrum from the whole remnant (it was accepted that the plasma is uniform and in collision ionization equilibrium (CIE)) yielded temperature $T = 1.2$ keV and column density $N_{\text{H}} = 2.8 \cdot 10^{20} \text{ cm}^{-2}$. The obtained parameters of RCW86 are given in Table 1. Pisarski et al. (1984) also showed that if this SNR is at the adiabatic stage of its evolution, it cannot be the result of the type II SN.

Nugent et al. (1984) analysed the spectrum of RCW86 (HEAO 1 experiment) with the assumptions: 1) that plasma emits in the CIE and, 2) for the first time, that the plasma is under nonequilibrium ionisation condition (NEI) with $T_e = T_i$. The best fitting of the CIE spectrum is for $T_{\text{high}} = 5.1 \pm 0.14$ keV, $T_{\text{low}} = 0.52 \pm 0.04$ keV, $N_{\text{H}} = (1.1 \pm 0.3) \cdot 10^{21} \text{ cm}^{-2}$. The NEI model gives $N_{\text{H}} = (4.4 \pm 0.3) \cdot 10^{21} \text{ cm}^{-2}$ and the parameters of the SNR shown in Table 1. The distance to RCW86 is smaller than to the OB-association but the authors have noted that the possible deviation from the NEI model may increase the distance to $d = 2.5$ kpc.

Claas et al. (1989) also used both the CIE and the NEI model for the interpretation of EXOSAT observation of RCW86. The possible contamination by the galactic ridge which increases the flux above 6 keV was subtracted, so in the two-component spectral model the smaller $T_{\text{high}} = 3.4 \pm 0.2$ keV was obtained. The low temperature component is believed to be a NEI effect. In this paper the parameters of RCW86 were also estimated using the surface brightness distribution. Higher emission from the SW part must be caused by a more dense ISM. Therefore, the Sedov (1959) solution is used only for the interpretation of the northeastern (NE) part of the SNR. The NEI model yields $T_s = T_e/1.3 = T_{\text{high}}/1.3 = (3.03 \pm 0.2) \cdot 10^7$ K.

ASCA X-ray data of RCW86 are considered by Vink et al. (1997). The authors reveal a remarkable temperature variation over the SNR: $T_e = 0.8 \div 5$ keV. They estimate the preshock density contrast for the SW and NE parts of RCW86 as $5 \div 50$ times.

Modelling the SNR emission it is necessary to take into consideration the possibility that the plasma may be under the NEI conditions, since the effects of the NEI are important. At the same time the nonuniformity of the surrounding ISM is very important, too. Calculations show that the influence of a nonuniform medium on the evolution and the properties of the emission of adiabatic SNRs may exceed the influence of the NEI in $10^1 \div 10^5$ times (Hnatyk & Petruk 1998, hereafter Paper I). At present it is practically impossible to construct models which take

into account both the NEI plasma emission effects and the ISM density gradient. Therefore, previous studies of RCW86 are based on the one-dimensional Sedov (1959) solution which cannot restore the observed morphology of the SNR. In this paper we show that the global anisotropy of the surface brightness distribution of RCW86 may be explain as a consequence of the SNR evolution in the ISM with a large-scale density gradient. We do not involve into the analysis the small-scale emission structures which are seen on the SNR's maps, because these structures are responsible for the local rises and do not essentially modify the global behaviour of the surface brightness. The plasma emission model used here is CIE.

2. The 2-D Modelling of RCW86

2.1. Method and models

Evolution of the SNR in the medium with a large-scale density distribution is taken as the principal basis for the models presented in this paper. We accept here spherically symmetrical energy emission during a SN explosion. We assume that the nonspherical shape and the global regular surface brightness anisotropy of the SNR is caused only by the *large-scale* structure of nonuniform medium.

The new model parameters associated with orientation of the SNR and his projection on the plan of the sky appear when 3D modelling executes. Projection effects complicate the analysis of the observations. In general case, it is impossible to reproduce unambiguously the real 3D shape for the knowing projection. In case of considered here the axis-symmetrical models, projection effects can easily be included into model. Simple connections between the parameters of the model and the projection exists. The angle δ between the symmetry axis of the 2D SNR and the visual cross-section is a new additional free parameter of the model.

At our previous paper (*Paper I*) it have been described a new approximate analytical method which allows the modelling a point explosion in media with a large-scale density gradient. We apply this method here to the describing of an evolution of the SNR RCW86. The possibilities of the SN explosion in 185 A.D. and in the OB-association will be considered separately .

We take as the basic initial model's parameters the three observational results: the visual angular size of the SNR $\Theta \approx 40'$, the temperature of the plasma's hot component $T_{\text{high}} = 3.4 \pm 0.2$ keV, which correspond to corrected for the contribution of the galactic ridge emission spectrum from the whole SNR (Claas et al. 1989) and the surface brightness distribution profile along the symmetry axis of the SNR's image (Pisarski et al. 1984) (see Fig. 4, 7). This profile is sensitive to large-scale density distribution of ISM and allows to see the properties of the density gradient.

Table 1. Parameters of RCW86 derived from the X-ray observations. R is radius of the SNR, E_{51} is the energy of SN explosion in 10^{51} erg, n_{H}° is hydrogen number density of surrounding medium, M is swept up mass, M_{\odot} is the mass of Sun.

Hydrodynamics model ^a	PEM ^b	t , years	R , pc	d , kpc	E_{51}	n_{H}° , cm^{-3}	M , M_{\odot}	Ref. ^d
Free expansion (SN II)	<i>CIE</i>	1800	9	1.4	$0.1 \div 0.2$	$0.13 \div 0.25$	$7 \div 14$	[1]
Sedov (SN I)	<i>CIE</i>	1800	6.5	1.4	$0.1 \div 0.2$	0.3	5	[1]
Free expansion or Sedov	<i>NEI</i>	$400 \div 1900$	$2.5 \div 9$	$0.4 \div 1.6$	$0.1 \div 0.2$	$0.04 \div 0.2$	$0.1 \div 21$	[2]
Sedov for NE part of the SNR	<i>NEI</i>	1800	6.7	1.1	0.15	0.11 ^c	4.9	[3]

^a All model assumed uniform ISM (density of ISM $\rho^{\circ} = \text{const}$)

^b Plasma emission model

^c The hydrogen number density of the ISM for the SW part is estimated as $(n_{\text{H}}^{\circ})_{\text{SW}} \sim 10(n_{\text{H}}^{\circ})_{\text{NE}}$

^d Reference: [1] – Pisarski et al. (1984); [2] – Nugent et al. (1984); [3] – Claas et al. (1989).

These characteristics are supplemented additionally with the fourth one depending on the one from two basic assumptions: the first assumption is that RCW86 is a result of the SN explosion in 185 A.D. (that gives the age of the SNR) and the second one is that RCW86 is a result of the SN explosion in the OB-association (this yields the distance to the SNR).

The temperature T_{s} at the shock front in the Sedov (1959) model of the SNR may be obtained from T_{high} : $T_{\text{s}} \approx T_{\text{high}}/1.3$ (Itoh 1977). In Paper I it have been shown that the nonspherical SNR may be characterised by the some "average" characteristic temperature $T_{\text{ch}} \propto (M)^{-1}$, which will be likely connected with T_{high} :

$$T_{\text{ch}} \approx T_{\text{high}}/1.3 = (3.03 \pm 0.2) \cdot 10^7 \text{ K}. \quad (1)$$

We have also shown that during the adiabatic stage the value of T_{ch} is close to T_{s} of the Sedov SNR with the same initial model parameters (e.g., the energy of explosion E_o , the hydrogen number density in the place of explosion $n_{\text{H}}^{\circ}(0)$) with the maximal error about $20 \div 30\%$. Therefore, we may write analogously to the Sedov case that

$$T_{\text{ch}} \approx T_{\text{s}} = 2.08 \cdot 10^{11} \left(\frac{E_{51}}{n_{\text{H}}^{\circ}(0)} \right)^{2/5} t_{\text{yr}}^{-6/5} \text{ K}, \quad (2)$$

$$T_{\text{ch}} \approx 6.47 \cdot 10^9 \left(\frac{E_{51}}{n_{\text{H}}^{\circ}(0)} \right) (\bar{R}_{\text{pc}})^{-3} \text{ K}, \quad (3)$$

where $E_{51} = E_o \cdot 10^{-51}$, t_{yr} is the age of the SNR in years, \bar{R}_{pc} is the average radius of the nonspherical SNR in pc. Hereafter $\gamma = 5/3$.

For the calculation of the X-ray emission of the plasma in the CIE the Raymond & Smith (1977) data were approximated.

2.2. RCW86 as the result of the SN explosion in 185 A.D.

2.2.1. Exponential medium

Let us take as initial SNR characteristics the angular size Θ , the temperature T_{ch} , the surface brightness profile and additionally the age of the SNR $t = 1800$ years.

We will consider the evolution of the SNR in the nonuniform medium with the flat exponential density distribution

$$\rho^{\circ}(r, \theta) = \rho^{\circ}(0) \exp\left(-\frac{r}{H} \cos \theta\right), \quad (4)$$

where $\rho^{\circ}(0)$ is the initial density around the place of SN explosion, H is the scale of the density nonuniformity, θ is an angle between the maximal density decreasing direction and the considered direction. Such exponential distribution is the one of the most possible to approximate real continuous density distributions in interstellar clouds, gaseous galactic disc etc.

When we fixed T_{ch} and t we have got from (2) an estimation on

$$E_{51}/n_{\text{H}}^{\circ}(0) = 1.5 \pm 0.25. \quad (5)$$

From this relation and appropriate explosion energy range $E_{51} = 0.1 \div 1$ the range for the initial number density $n_{\text{H}}^{\circ}(0) = 0.06 \div 0.8 \text{ cm}^{-3}$ follow.

From the definition of a dimensionless time (Hnatyk & Petruk 1996) $\tau = t/t_{\text{m}}$ with $t_{\text{m}} = \alpha_{\text{A}}^{1/2} E_o^{-1/2} \rho_o^{1/2}(0) R_{\text{m}}^{5/2}$ (where α_{A} is the self-similar constant, R_{m} is the distance scale) it is obtained for $\gamma = 5/3$ that

$$t = \tau t_{\text{m}} = 18.01 \left(\frac{E_{51}}{n_{\text{H}}^{\circ}(0)} \right)^{-1/2} R_{\text{m,pc}}^{5/2} \tau \text{ yr}, \quad (6)$$

$R_{\text{m,pc}}$ is the distance scale in pc.

From this relation and (5) a connection between the scale high H and the dimensionless time follows:

$$H = R_{\text{m}} \simeq (6.8 \pm 0.2) \cdot \tau^{-2/5} \text{ pc}. \quad (7)$$

The possible values of H lie in the range $H = 150$ pc for the Galactic's disk to few parsecs for a local nonuniformity of the ISM. The influence of the nonuniform medium on the dynamics of the SNR become more appreciable with the age of a SNR. The surface brightness distribution of a SNR will be close to the Sedov one for small τ . Since the observational distribution of the surface brightness in

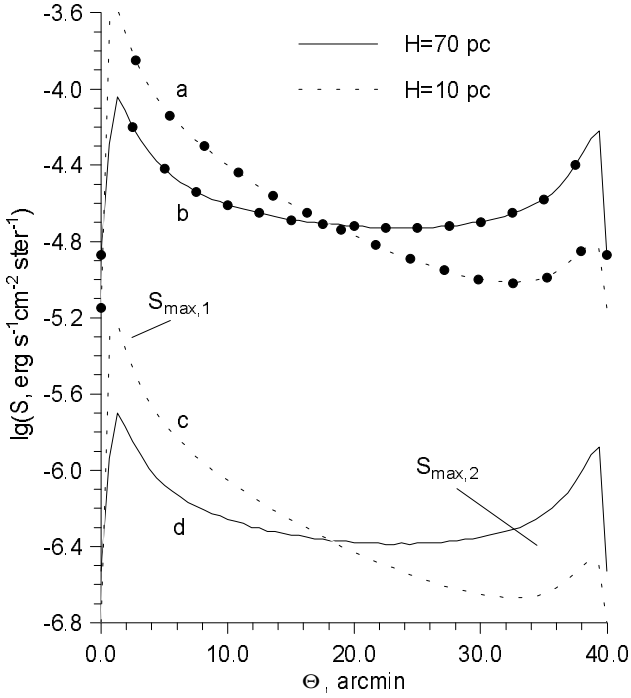


Fig. 1. Surface brightness S distribution in the diapason $\varepsilon = 0.1 \div 2$ keV along the median of the SNR in the ISM with the exponential density distribution (4) for the four cases of the initial model parameters. It is suppose here for all cases that $E_{51}/n_{\text{H}}^o(0) = 1.5$, $H_{\text{pc}}\tau^{2/5} = 6.85$, $t = 1800$ years and $T_{\text{ch}} = 3.0 \cdot 10^7$ K. Solid lines show the cases with $H = 70$ pc, dashed – the cases with $H = 10$ pc. Energies of explosion: a, b: $E_{51} = 1$; c, d: $E_{51} = 0.15$. Dots represent the cases c, d multiplied by the factor $((n_{\text{H}}^o(0))_{\text{top}}/(n_{\text{H}}^o(0))_{\text{bottom}})^2 = 10^{1.66}$.

RCW86 is not similar to the Sedov one, the dimensionless time τ have not to be small.

The observed ratio ξ between the axes of the visual shape of RCW86 is in range $\xi = 1.0 \div 1.2$ (Pisarski et al. 1984). This corresponds to ranges of $\tau = 0.01 \div 11$ (Fig. 5 in Paper I). The scale height H , as it follow from (7), then must be anywhere between 2.6 and 40 pc. Such wide range of H is a result of very slow decreasing of the visual shape's anisotropy with time (the same Fig.). Small scale height (like $H = 2.6$ pc) it seems to be impossible because the surface brightness contrast then must be about $10^{4.7}$ times. Possible presence in the shape anisotropy the residual component related to anisotropy which the SNR might have on the free expansion stage (due to aspherical explosion) is the second reason which complicates using the small anisotropy of the shape for estimating the H and τ .

Physically the most correct limitation on H and τ we may get from the profiles of the surface brightness. In Fig. 1 are shown the profiles of the surface brightness for the four cases of the initial model parameters. Relations (5) and (7) have place for each set of the parameters. We may see that for fixed H and τ the shape of the profile

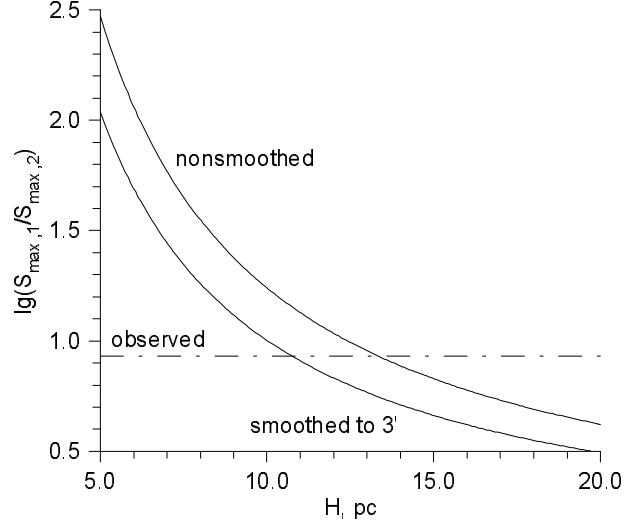


Fig. 2. Ratios of the values of the two peaks in the surface brightness S distribution versus the high scale H for models of SNR in the flat exponential media (4). Here $t = 1800$ years and $E_{51}/n_{\text{H}}^o(0) = 1.5$. In the figure both contrast of surface brightness are shown: smoothed to $3'$ like observed (Pisarski et al. 1984) and without smoothing.

is the same. Value of the blast energy E_{51} (and as consequence of (5), the number density $n_{\text{H}}^o(0)$) give the amplitude of the profile which may differ with the factor about few ten times. It is follow from Fig. 1 that the values H and τ affect on the contrast of the surface brightness.

For finding H , it is possible to accept the contrast between the brightness in the different points of the SNR's image. For example, it may be used the relation between the two "near-front" maximums in the distribution. The most appropriate value of high scale for this choice, as it may be seen from Fig. 2, is $H = 11.0$ pc (and respectively $\tau = 0.3$). Then calculations show (Fig. 4) that the most appropriate value of the blast energy is $E_{51} = 0.22$ ($n_{\text{H}}^o(0) = 0.15 \text{ cm}^{-3}$).

For normalizing the surface brightness S in photon energy range $\varepsilon = 0.1 \div 2.0$ keV, the effective values of photon energy $\bar{\varepsilon} = 0.1$ keV and absorption cross section $\bar{\sigma}$ as cross section at photon energy $\varepsilon = 0.316$ keV from Morrison & McCammon (1983) have been used.

Obtained SNR's luminosity $L_x^{0.1-2} = 3.5 \cdot 10^{34}$ erg/s is consistent with established by Pisarski et al. (1984) $L_x^{0.2-4} = 2 \cdot 10^{34} d_{\text{kpc}}^2$ erg/s.

In Fig. 5 it is shown the maps of the surface brightness distribution for this model in comparison with the distribution of the spectral index $\alpha = -\partial \ln F_{\varepsilon} / \partial \ln \varepsilon$, where F_{ε} is the continuum flux at photon energy ε .

2.2.2. Power law medium

It is useful to note, that concrete appearance of surrounding density distribution is not strongly essential then size

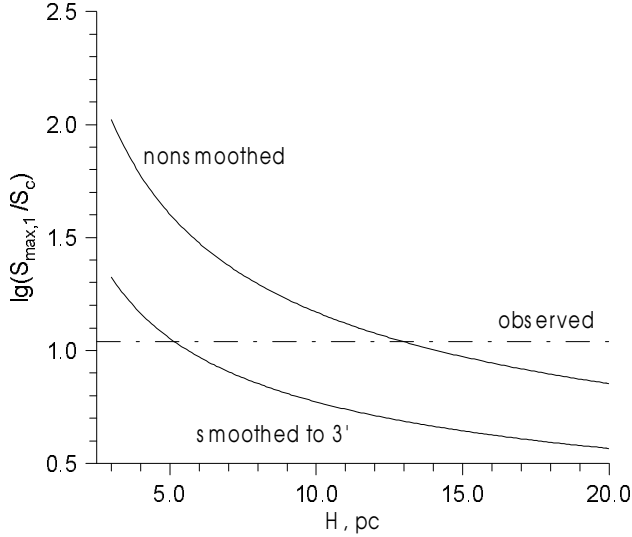


Fig. 3. The same as in Fig. 2 for the ratios between the maximum in the surface brightness distribution $S_{max,1}$ and the value of the brightness in the visual geometric center of the SNR S_c .

of SNR does not exceed a few scale heights. Namely, similar parameters of model may be obtained under assumption that the SNR evolve in other type of media, if contrast of density along the surface of the SNR will be similar. Let us consider, for example, a medium with the spherically-symmetrical power law density distribution created by stellar wind

$$\rho^o(\tilde{r}) = \rho_o(\tilde{r}/R_m)^\omega, \quad (8)$$

then the SN explosion position is displaced on the distance r_o from the center of symmetry $\tilde{r} = 0$, therefore, the density distribution as a function of the distance r from the explosion point $r = 0$ is:

$$\rho^o(r, \theta) = \rho^o(0) \left(\frac{\sqrt{r_o^2 + r^2 + 2rr_o \cos \theta}}{r_o} \right)^\omega. \quad (9)$$

We take $\omega = -2$ and calculate a number of models in order to get an appropriate r_o using the surface brightness contrast between the two maximums in the brightness distribution.

Observed surface brightness contrast is obtained in this model with $r_o = 21.8$ pc. Characteristic scale H_{ch} for medium (9) with such r_o may be estimated. It equals $H_{ch} = 11$ pc. Other parameters of the model are really close to the same parameters of the SNR in exponential medium (4) and shown in Tables 2 and Fig. 4.

2.2.3. Exponential plus uniform medium

RCW86 may evolve in the ISM with the contact between the uniform medium $\rho^o = \text{const}$ and the region with the

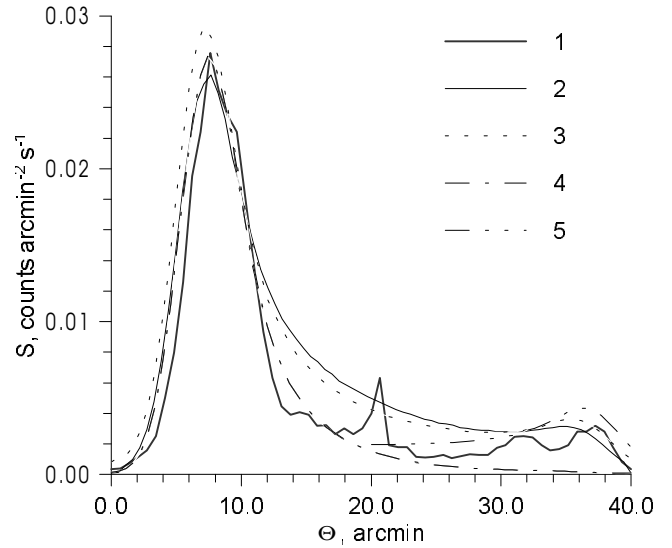


Fig. 4. Observed (line 1) distribution of the surface brightness S along of the symmetry axis of RCW86 (Pisarski et al. 1984) and the distributions in the models of SNRs with the age $t = 1800$ years: line 2 – the exponential medium (4) with $H = 11$ pc and $E_{51} = 0.22$, $n_H^o(0) = 0.15 \text{ cm}^{-3}$; line 3 – the power law medium (9) with $r_o = 21.8$ pc and the same E_{51} , $n_H^o(0)$; line 4 – the exponential medium (4) with $H = 5$ pc and $E_{51} = 0.17$, $n_H^o(0) = 0.11 \text{ cm}^{-3}$; line 5 – the uniform medium, $E_{51} = 0.17$, $n_H^o = 0.11 \text{ cm}^{-3}$. All distributions are smoothed to $3'$.

higher density (e.g., interstellar cloud) where density is distributed according to the exponential law (4). In this case one part of the SNR (the NE part of RCW86) will evolve in the uniform medium whereas the evolution of the another part (the SW part of RCW86) will be determined by the variation of the density in the dense region. In this composite model the surface brightness in the central part of the SNR will be close to the brightness which the Sedov model gives, but the maximal brightness will be determined by the concrete distribution of the density in the nonuniform region.

When we take as initial parameter the ratio of the maximum of the brightness distribution to the value of the brightness in the visual geometrical centre of the SNR, we obtaine another model parameters for the case of the exponential law density distribution, namely, $H = 5.0$ pc (Fig. 3) and $E_{51} = 0.17$ (Fig. 4). We may calculate now the profile of the surface brightness for the Sedov model wich describes the NE part of RCW86 in the assumption of the composite medium (Fig. 4). The initial parameters for it are the same as for the SW part, $E_{51} = 0.17$, $n_H^o(0) = 0.11 \text{ cm}^{-3}$. We may see that the composite medium model (exponential plus constant density distributions) more better describes the observational surface brightness distribution than the exponential medium alone.

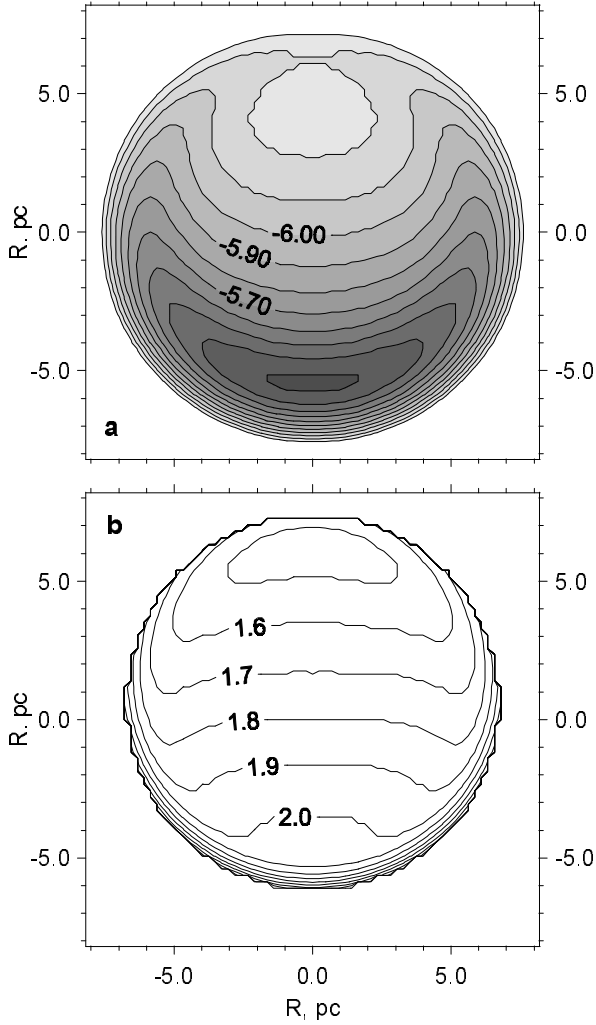


Fig. 5. **a** The surface brightness S (in $\text{erg s}^{-1} \text{cm}^{-2} \text{st}^{-1}$) distribution in the photon energy range $\varepsilon = 0.1 - 2$ keV. **b** The surface brightness distribution of the spectral index α at $\varepsilon = 5$ keV for the SNR model in the exponential medium (4) with $H = 11.0$ pc. Parameters of the model are $t = 1800$ years, $E_{51} = 0.22$, $n_{\text{H}}^{\circ}(0) = 0.15 \text{ cm}^{-3}$ and $\delta = 0^{\circ}$.

It is necessary to note, when RCW86 is the SNR created by the explosion in 185 A.D., we see it near the maximum disclosing projection ($\delta \approx 0^{\circ}$). Really, another projections hide the real contrasts (e.g., of axes size, surface brightness; see Paper I). If we see the contrast of surface brightness decreased already, then the real one must be greater and therefore H must be smaller.

Obtained parameters of RCW86 are summarised in Table 2 (the first three columns).

2.3. RCW86 as the result of the SN explosion in the OB-association

Let us suppose now that RCW86 is a result of the SN explosion in the OB-association which distance from us is

Table 2. Parameters of RCW86 obtained from the different models of the SNR. Plasma emission model is CIE. L_{x} is in the photon energy range $\varepsilon = 0.1 \div 2.0$ keV. $R(0)$ and $R(\pi)$ are the radii of shock in directions $\theta = 0$ and $\theta = \pi$ respectively, D is the shock velocity.

Parameters of model	Initial density distribution				
	E ^a	PL ^b	EU ^c	E ^a	E ^a
<i>Observed</i>					
Θ , arcmin	40	40	40	40	40
T_{ch} , 10^7 K	3.0	3.0	3.0	3.0	3.0
<i>Additionally supposed</i>					
t , years	1800	1800	1800	—	—
d , kpc	—	—	—	2.8	2.8
H , pc	11	$\sim 11^d$	5.0	26	22
δ , degree	0	0	0	0	30
<i>Obtained</i>					
t , years	1800	1800	1800	4300	4300
E_{\circ} , 10^{51} erg	0.22	0.22	0.14	2.0	2.0
$n_{\text{H}}^{\circ}(0)$, cm^{-3}	0.15	0.15	0.10	0.1	0.1
$R(0)$, pc	7.50	7.42	6.84	17.96	18.25
$R(\pi)$, pc	6.27	6.20	5.78	14.96	14.78
$D(0)$, km/s	1800	1740	1490	1810	1870
$D(\pi)$, km/s	1260	1220	1070	1250	1230
$T(0)$, 10^7 K	4.45	4.18	3.03	4.50	4.82
$T(\pi)$, 10^7 K	2.17	2.03	1.58	2.16	2.07
$n_{\text{H}}^{\circ}(R, 0)$, cm^{-3}	0.08	0.08	0.10	0.18	0.19
$n_{\text{H}}^{\circ}(R, \pi)$, cm^{-3}	0.27	0.29	0.31	0.05	0.04
d , kpc	1.18	1.17	1.08	2.83	2.83
M , M_{\odot}	6.9	6.8	—	62	62
$\lg(L_{\text{x}}, \text{erg/s})$	34.54	34.53	—	35.33	35.35
$\alpha(5 \text{ keV})$	1.90	1.88	—	1.91	1.92

^a E is the flat exponential medium (4)

^b PL is the power law medium (9) with $\omega = -2$ and $r_o = 21.8$ pc

^c EU is the exponential medium (4) plus uniform

^d Characteristic scale height H_{ch}

estimated (e.g., Westerlund 1969). In this section the next question is the main: what scale height has the medium around the RCW86 if the SNR's progenitor have exploded in this OB-association? Therefore the nonuniform media with exponential density distribution (4) is used.

We take as the initial SNR characteristics the observational angular size Θ , the temperature T_{ch} , the surface brightness profile and, additionally, the distance to the remnant $d \approx 2.8 \pm 0.4$ kpc (Rosado et al. 1996).

It is possible now to estimate the average SNR's radius from Θ and d : $\bar{R}_{\text{pc}} = 0.5d_{\text{kpc}}\Theta'/3.438 \approx 16.3 \pm 2.3$ pc. Therefore we have got from (3) an estimation on

$$E_{51}/n_{\text{H}}^{\circ}(0) \simeq 23 \pm 10. \quad (10)$$

This means that the explosion energy must be high and the initial number density have to be low.

The age of the SNR as it follows from (2) is anywhere from $t = 3500$ years for $T_{\text{ch}} = 2.8 \cdot 10^7$ K and

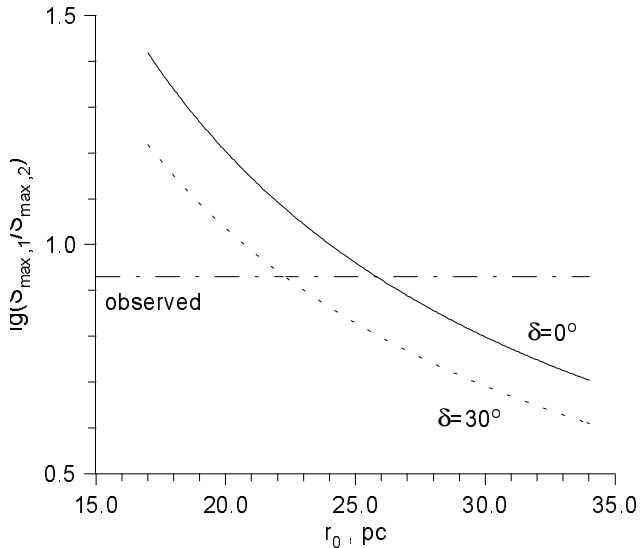


Fig. 6. Ratios of the values of the two peaks in the X-ray surface brightness S distribution versus H for the SNRs in the exponential media (4), when $t = 4300$ years, $E_{51}/n_{\text{H}}^o(0) = 20.3$ and $\delta = 0^\circ$. Dashed line is the same relation for the same SNR models, except $\delta = 30^\circ$. All ratios are smoothed to $3'$.

$E_{51}/n_{\text{H}}^o(0) = 13$, up to $t = 5350$ years in case $T_{\text{ch}} = 3.2 \cdot 10^7$ K and $E_{51}/n_{\text{H}}^o(0) = 32$. We may see, with agreement with Rosado et al. (1996), if RCW86 is the remnant of the SN exploded in OB-association it can not be borned in 185 A.D.

For the distance $d = 2.8$ kpc and $T_{\text{ch}} = 3.0 \cdot 10^7$ K the age $t = 4300$ years and ratio $E_{51}/n_{\text{H}}^o(0) = 20.3$ have been obtained. We calculate the evolution of RCW86 in the exponential medium (4) with these initial parameters.

It may be seen from Fig. 6 that the scale height $H = 25.7$ pc is the most appropriate for the case of the maximal disclosure of the remnant ($\delta = 0^\circ$).

In order to estimate an explosion energy E_o and a number density $n_{\text{H}}^o(0)$ it was calculated a number of the models with such H and different E_o . It may be seen from Fig. 7 that the surface brightness distribution along the symmetry axis for $E_{51} = 2.0$, $n_{\text{H}}^o(0) = 0.1 \text{ cm}^{-3}$ is near of the observed one. The whole maps of the surface brightness S and the spectral index α distribution are shown in Fig. 8.

Fig. 7 demonstrates also the surface brightness distribution along the symmetry axis for the case of the different projection of the SNR, when $\delta = 30^\circ$. We see that distribution, like observational, may be obtained also under different projection of the 2D SNR on the plan of the sky with the smaller $H = 22.3$ pc. Now we cannot separate one case of projection from another but we see also that the model with $\delta = 30^\circ$ does not essentially change the SNR's parameters which are summarised for these different models of RCW86 in the last two columns of Table 2.

Modelling reveal also that for model with $\delta = 30^\circ$ both the surface brightness distribution and the surface distri-

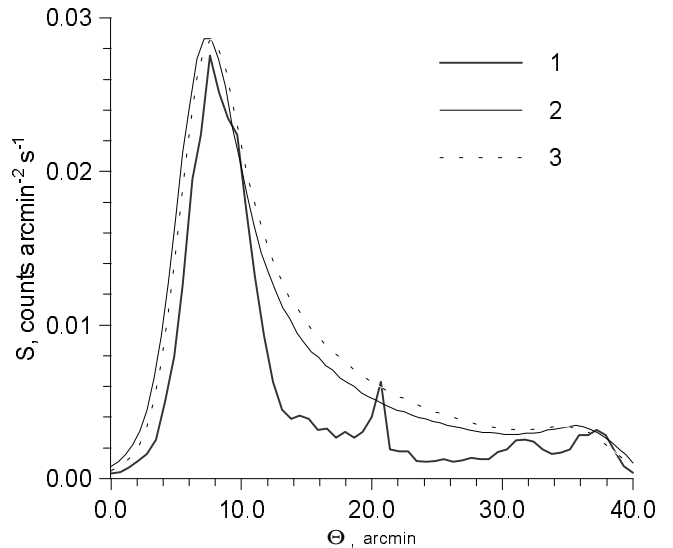


Fig. 7. Distribution of the surface brightness S along the symmetry axis of the SNR RCW86: line 1 – observational (Pisarski et al. 1984); line 2 – model in exponential medium (4) with $H = 25.7$ pc and $t = 4300$ years, $E_{51} = 2.0$, $n_{\text{H}}^o(0) = 0.1 \text{ cm}^{-3}$, $\delta = 0^\circ$; line 3 – the same model, except $H = 22.3$ pc and $\delta = 30^\circ$. All distributions are smoothed to $3'$.

bution of the spectral index are also very close to shown in Fig. 8 case of $\delta = 0^\circ$.

2.4. Contribution of the ejecta

Nugent et al. (1984) have made the conclusion that the observed data on RCW86 can be fitted without taking into consideration the emission from the ejecta. These authors have also suggested that the value of $\beta = M_{\text{ej}}/E_{51}$ (M_{ej} is the mass of ejecta in M_\odot) lies much probably in the range 1 to 10. In our models of the SNR the blast energy are $E_{51} = 0.22$ in the case of SN explosion in A.D.185 and $E_{51} = 2.0$ in the case of SN explosion at a distance $d = 2.8$ kpc. Therefore, the mass of ejecta may be estimated as $M_{\text{ej}} = 0.22 \div 2.2M_\odot$ or $M_{\text{ej}} = 2 \div 20M_\odot$. Swept up masses are respectively 7 and 62 M_\odot and exceeds M_{ej} in 3 to 31 times. We expect that under our assumption of CIE conditions and obtained $n_{\text{H}}^o \sim 0.1 \text{ cm}^{-3}$, such swept up masses are enough for RCW86 to be in Sedov phase of his evolution. So, we may assume that in both cases the ejecta do not considerably modify the emission from RCW86. However, if to take into account the NEI effects and consider the value of the β up to the possible upper limit which have been put as $\beta \sim 40$, the contribution of the ejecta into the emission might be essential (Nugent et al. 1984). On the other hand, if RCW86 would evolve in very dense ISM ($n_{\text{H}}^o \sim 10^3$), it would entry in Sedov stage after sweeping up $M \sim 19M_{\text{ej}}$ (Dohm-Palmer & Jones 1996).

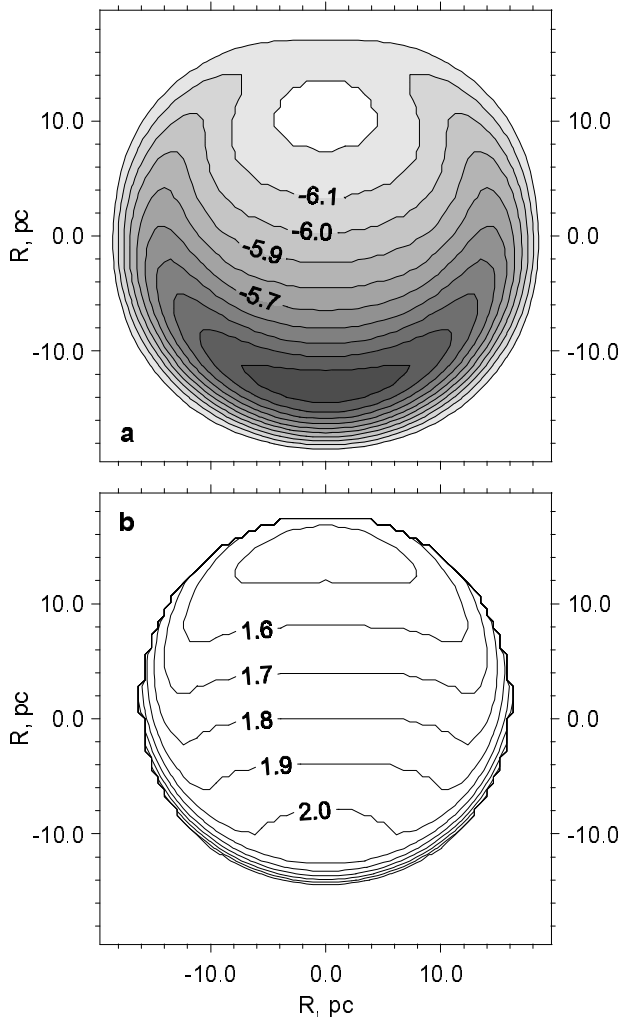


Fig. 8. **a** The surface brightness S (in $\text{erg s}^{-1} \text{cm}^{-2} \text{st}^{-1}$) distribution in the range $0.1 - 2$ keV and **b** the surface brightness distribution of the spectral index α at $\varepsilon = 5$ keV for the SNR model in the nonuniform exponential medium (4) with $H = 25.7$ pc. Parameters of the model are $t = 4300$ years, $E_{51} = 2.0$, $n_{\text{H}}^{\circ}(0) = 0.1 \text{ cm}^{-3}$ and $\delta = 0^{\circ}$.

3. Conclusions

Observations reveal complicated RCW86 morphology. Close to spherical shape of the SNR coexists with the surface brightness distribution which is far from the Sedov one. When we take into account the nonuniform ISM we may explain such morphology.

We considered here the 2-D models of RCW86 in a few types of nonuniform media. It is shown that the features of the surface brightness distribution allow us to restore the SNR characteristics. As it is described, the contrasts in the surface brightness depend on the gradient of the density of the ISM and the age of the SNR, whereas the amplitude of the surface brightness distribution depends on the energy of the Supernova explosion and the initial density around the place of explosion.

It is shown that observed surface brightness distribution of RCW86 may be obtained in the models with the two different initial assumptions: one about the Supernova explosion in 185 A.D. and another about the explosion in the OB-association. Data we possess do not allow us to decide which of those models is true. The parameters obtained for RCW86, basing on these two assumptions, are summarized in Table 2. The models give the observational contrasts of the surface brightness when we consider the ISM with the scales of nonuniformity 11 pc (if the age of RCW86 is 1800 years) or 20–25 pc (when the SNR is distant from us on 2.8 kpc). The preshock density contrasts between the southwestern and the northeastern parts of RCW86 in range 3.5–4.5 are obtained for both considered assumptions.

Acknowledgements. I am very grateful to Dr. Bohdan Hnatyk for the permanent attention to my work as well as for always useful advices.

References

- Caswell, J., Clark, D., Crawford, D. 1975, *Austr. Phys. Ap. Suppl.*, 37, 46
 Chin, Y.-N., Huang, Y.-L. 1994, *Nature*, 371, 398
 Claas, J., Smith, A., Kaastra, J., et al. 1989, *ApJ*, 337, 399
 Clark, D., Stephenson, F. 1977, *Historical Supernovae*, Pergamon, Oxford
 Dohm-Palmer, R., Jones, T. 1996, *ApJ*, 471, 279
 Itoh, H. 1977, *Pub. Astr. Soc. Japan*, 29, 813
 Hill, E. 1967, *Austr. J. Phys.*, 20, 297
 Hnatyk, B., Petruk, O. 1996, *Kinematics and Physics of Celestial Bodies*, 12, 35
 Hnatyk, B., Petruk, O. 1998, *A&A*, *in press* (Paper I)
 Klimishin, I. 1984, *Shock Waves in the Star Envelopes*, Nauka, Moscow
 Milne, D. 1970, *Austr. J. Phys.*, 23, 425
 Milne, D. 1987, *Austr. J. Phys.*, 40, 771
 Morrison, R., McCammon, D. 1983, *ApJ*, 270, 119
 Naranan, S., Shulman, S., Yentis, D. et al. 1977, *ApJ*, 213, L53
 Nugent, J., Pravdo, S., Garmire, G. et al., 1984, *ApJ*, 284, 612
 Pisarski, R., Helfland, D., Kahn, S. 1984, *ApJ*, 277, 710
 Raymond, J., Smith, B. 1977, *ApJS*, 35, 419
 Rosado, M., Ambrosio-Cruz, P., Le Coarer, E., et al., 1996, *A&A*, 315, 234
 Ruiz, M. 1981, *ApJ*, 243, 814
 Schaefer, B. 1995, *AJ*, 110, 1793
 Sedov, L. 1959, *Similarity and Dimensional Methods in Mechanics*, Academic, New York
 Strom, R. 1994, *MNRAS*, 268, L5
 van den Bergh, S. 1978, *ApJS*, 38, 120
 Vink, J., Kaastra, J., Bleeker, J. 1997, *A&A*, 328, 628
 Westerlund, B. 1969, *AJ*, 74, 879
 Winkler, P. 1978, *ApJ*, 221, 220
 Whiteoak, J.B., Green, A. 1996, *A&AS*, 118, 329